Video Article

A Phenotyping Regimen for Genetically Modified Mice Used to Study Genes Implicated in Human Diseases of Aging

Victoria L. Patterson*[1], Brian S. Thompson*[1], Catherine Cherry*[1], Shao-bin Wang[2], Bo Chen[2], Josephine Hoh[1,2]

[1]Department of Environmental Health Sciences, Yale University School of Medicine

[2]Department of Ophthalmology, Yale University School of Medicine

*These authors contributed equally

Correspondence to: Josephine Hoh at josephine.hoh@yale.edu

URL: https://www.jove.com/video/54136
DOI: doi:10.3791/54136

Keywords: Medicine, Issue 113, Parkinson's disease, age-related macular degeneration, mitochondria, HtrA1, HtrA2, HtrA3, HtrA4, complement factor H (CFH)

Date Published: 7/14/2016

Citation: Patterson, V.L., Thompson, B.S., Cherry, C., Wang, S.b., Chen, B., Hoh, J. A Phenotyping Regimen for Genetically Modified Mice Used to Study Genes Implicated in Human Diseases of Aging. *J. Vis. Exp.* (113), e54136, doi:10.3791/54136 (2016).

Abstract

Age-related diseases are becoming increasingly prevalent and the burden continues to grow as our population ages. Effective treatments are necessary to lessen the impact of debilitating conditions but remain elusive in many cases. Only by understanding the causes and pathology of diseases associated with aging, can scientists begin to identify potential therapeutic targets and develop strategies for intervention. The most common age-related conditions are neurodegenerative disorders such as Parkinson's disease and blindness. Age-related macular degeneration (AMD) is the leading cause of blindness in the elderly. Genome wide association studies have previously identified loci that are associated with increased susceptibility to this disease and identified two regions of interest: complement factor H (CFH) and the 10q26 locus, where the age-related maculopathy susceptibility 2 (ARMS2) and high-temperature requirement factor A1 (HtrA1) genes are located. CFH acts as a negative regulator of the alternative pathway (AP) of the complement system while HtrA1 is an extracellular serine protease. ARMS2 is located upstream of HtrA1 in the primate genome, although the gene is absent in mice. To study the effects of these genes, humanized knock-in mouse lines of *Cfh* and *ARMS2*, knockouts of *Cfh*, *HtrA1*, *HtrA2*, *HtrA3* and *HtrA4* as well as a conditional neural deletion of *HtrA2* were generated. Of all the genetically engineered mice produced only mice lacking HtrA2, either systemically or in neural tissues, displayed clear phenotypes. In order to examine these mice thoroughly and systematically, an initial phenotyping schedule was established, consisting of a series of tests related to two main diseases of interest: AMD and Parkinson's. Genetically modified mice can be subjected to appropriate experiments to identify phenotypes that may be related to the associated diseases in humans. A phenotyping regimen with a mitochondrial focus is presented here alongside representative results from the tests of interest.

Video Link

The video component of this article can be found at https://www.jove.com/video/54136/

Introduction

Age-associated diseases are becoming increasingly prevalent in modern society. As medical science improves and life expectancy increases, the population continues to age and the burden of these diseases grows. Effective treatments are necessary to lessen the impact of debilitating conditions but remain elusive in many cases. Only by understanding the causes and pathology of diseases associated with aging can scientists begin to identify potential therapeutic targets and develop strategies for intervention. Common age-related conditions include neurodegenerative disorders such as Parkinson's disease (PD) and age-related macular degeneration (AMD). PD is the most common movement disorder caused by neurodegeneration in humans. Most PD patients show symptoms such as resting tremor, bradykinesia and rigidity after 50 years of age. Early onset has also been observed in approximately 10% of cases.

AMD is the leading cause of blindness in the elderly, progressively damaging photoreceptors and the retinal pigment epithelium (RPE) in the eye. Central vision is impaired but the peripheral vision is generally unaffected. There are two forms of AMD. In the "dry" form, extracellular protein deposits known as drusen form between the RPE and Bruch's membrane (BM), leading to geographic atrophy and blurring of central vision. The more severe "wet" form results from neovascularization from the choroid across BM into the RPE and photoreceptor layers and can lead to hamorrhaging beneath the retina that causes permanent damage to retinal tissue. Genome wide association studies have previously identified loci that are associated with increased susceptibility to this disease and identified two regions of interest: complement factor H (CFH) on chromosome 1 and the 10q26 locus, where the age-related maculopathy susceptibility 2 (ARMS2) and high-temperature requirement factor A1 (HtrA1) genes are located[1-5]. Combinations of these alleles increase the likelihood of AMD in a dose dependent manner and specific SNPs can be preferentially associated with either the wet or dry forms of AMD[3-6].

CFH acts as a negative regulator of the alternative pathway (AP) of the complement system by inhibiting the activation of C3. A single nucleotide polymorphism (SNP) has been linked to increased risk of AMD, causing exchange of tyrosine 402 in exon 9 with histidine due to a T to C

substitution[1]. In AMD it is believed that the AP is misregulated because of a loss of function of CFH but whether the SNP plays a causal role is unclear. One hypothesis is that the positively charged histidine is thought to negate the ability of CFH to bind to interacting proteins C-reactive protein and heparin sulfate[1,7]. *In vitro* studies of CFH Y402H provide conflicting results over functional differences between the variants, and *in vivo* work in *Cfh*$^{-/-}$ mice expressing humanized CFH is ongoing[8]. ARMS2 is located upstream of HtrA1 in the primate genome, although the gene is absent in mice. HtrA1 is a serine protease but ARMS2 is poorly characterized. The linkage disequilibrium between SNPs in the AMD-associated locus has made it difficult to determine the contributions to risk of individual mutations of the genes in this region, but recent work has suggested that it is overexpression of HtrA1 rather than ARMS2 that leads to neovascularization and subretinal protein deposits[9-11]. However, the close proximity of the genes in this locus may allow for interactions that cannot be studied using randomly inserted transgenes.

In addition to AMD, the HtrA family of serine proteases has been associated with many human diseases. All HtrA proteins contain a serine protease domain followed by at least one C-terminal PDZ domain. HtrA1, HtrA3 and HtrA4 share the greatest homology, consisting of a signal peptide, insulin-like growth factor binding domain, a Kazal protease inhibitor domain, the serine protease domain and a PDZ domain. HtrA2 has a different N-terminus, composed of a mitochondrial localization sequence, transmembrane domain and inhibitor of apoptosis binding domain followed by the protease and PDZ domains[12-16]. Mammalian HtrA1 is regulated by substrate-induced remodeling in the active site of its protease domain[17-20], and HtrA2 can also be modulated by interaction between the serine protease and PDZ domains that suppresses protease activity[21]. Interestingly, the PDZ domain does not appear to confer similar regulation to HtrA3[16]. The HtrA proteases can also be regulated by extrinsic factors: it was recently demonstrated that there exists a regulatory interaction between HtrA1 and protoporphyrins[22] and HtrA2 can be regulated by phosphorylation upon activation of the p38 MAP kinase pathway in a PINK1-dependent manner[23]. The deletion of individual members of the HtrA family in mice has been documented, however mechanistic effects mostly are unclear partly due to lack of visible phenotypes.

HtrA1 plays an important function in protein quality control and its misregulation or mutation has been associated with many different human diseases including arthritis, cancer and an increased risk of AMD[3,4,24-32]. Loss of HtrA2 function in neural tissues has been associated with PD phenotypes in humans and mice, while its loss from non-neural tissues results in accelerated aging[33-37]. HtrA3 dysregulation has been associated with diseases including preeclampsia and certain types of cancer[38,39]. Up-regulation of HtrA4 has been observed in the placentas of preeclampsia patients but knockout mice do not display an overt phenotype[40,41]. The lack of phenotypes observed in some knockout mice has been postulated to be a result of compensation between the HtrA family member: it is thought that both HtrA4 and HtrA1 interact with the TGF-B family of proteins, allowing for compensation by HtrA1 upon deletion of HtrA4[41]. Similarly, it is thought that since HtrA1 and HtrA3 have a high degree of domain homologies they might have complementary functions[42]. However, it has been suggested that HtrA proteins may have partially antagonistic roles, competing to regulate common targets[43].

To further investigate these risk factors three humanized knock-in mouse lines were generated. In *Cfh*$^{tm1(CFH*9)jhoh}$ and *Cfh*$^{tm2(CFH*9)jhoh}$, exon 9 of the *Cfh* gene is replaced with exon 9 of the human homologue. *Cfh*$^{tm1(CFH*9)jhoh}$ encodes the non-disease associated tyrosine residue at position 402, whereas *Cfh*$^{tm2(CFH*9)jhoh}$ carries the Y402H, risk-associated SNP. In *ARMS2*^{tm1jhoh} the human ARMS2 sequence was targeted to a region upstream of HtrA1. A loxP-flanked STOP sequence placed upstream of the gene sequence but downstream of the included UbiC promoter was excised by crossing to OzCre mice, which express Cre recombinase under the control of the Rosa26 promoter, as previously described[34]. In addition to these knock-in lines, conditional knockout alleles for *Cfh* and *HtrA1* (*Cfh*^{tm1jhoh} and *HtrA1*^{tm1jhoh}), as well as the other known HtrA family members were generated: *HtrA2* (*HtrA2*^{tm1jhoh}), *HtrA3* (*HtrA3*^{tm1jhoh}) and *HtrA4* (*HtrA4*^{tm1jhoh}). The germ-line knockouts were created by crossing OzCre mice to animals engineered to flank specific exons with loxP sites, such that deletion causes a frame shift and/or deletion of the active domain (*Cfh*; exon 3, *HtrA1*; exons 2-3, *HtrA2*: exons 2-4, *HtrA3*; exon 3, *HtrA4*; exons 4-6)[34,41]. A neural deletion of HtrA2, deleted using Cre recombinase under control of the *Nestin* promoter (*HtrA2*^{flox};Tg(Nes-cre)1Kln/J), has also been described[34]. Only mice lacking HtrA2, either systemically or in neural tissues, displayed clear phenotypes, presenting with Parkinsonian phenotypes.

Since some of these genes of interest are posited to be localized to mitochondria[11,44-47], and deletion of HtrA2 generated Parkinsonian phenotypes, a phenotyping regimen with a mitochondrial and neurological focus is described here and representative results from the tests of interest are provided. In order to examine genetically engineered mice produced to investigate human, age-related disease thoroughly and systematically an initial phenotyping schedule was established, consisting of a series of tests related to the two main diseases of interest: AMD and Parkinson's.

Protocol

Ethics statement: Studies involving animals were conducted in compliance with the National Institutes of Health recommendations in the Guide for the Care and Use of Laboratory Animals and Institutional Animal Care and Use Committee (IACUC) at Yale University.

1. Behavioral Testing of Genetically Modified Mice

Note: All mice should be subjected to the same testing regimen to limit differences in habituation to handling. Tests should be performed at the same time of day each time.

1. Neonatal Hind Limb Test
   Note: The hind limb test is conducted daily from postnatal day (P) 4 to P10 to evaluate proximal hind limb muscle strength, weakness and fatigue.
   1. Transport mice to testing area and allow to rest for 30 min before testing.
   2. Prepare testing apparatus by cleaning a 50 ml conical tube with 70% ethanol, pushing two (P4-P8) or one (P9-P10) cotton balls to the bottom of the tube and securing in a vertical position.
   3. Remove one pup from the cage and record weight. Keep pup in holding tray on heat pad whenever not testing.
   4. Gently suspend the hind limbs of the neonate over the rim of the conical tube, such that it is facing down towards the cotton balls. Count the number of pull attempts made and measure latency to fall using a stopwatch.
   5. Repeat once more then label the pup with marker. Afterwards, identify P6 pups by toe clipping. Rub pups gently with bedding from home cage before replacing.

6. Wipe conical tube with 70% ethanol.
7. Repeat testing on next pup until the whole litter has been tested.
8. Dispose of cotton ball and conical tube. Clean all equipment with 70% ethanol.

2. Weanling Observation Test
Note: The weanling observation test is administered daily from P19 to P21 to score movement and general activity levels.
1. Transport mice to testing area and allow to rest for 30 min before testing.
2. Prepare Plexiglas testing box marked with a 6x6 grid of 2 inch squares on the base by cleaning with 70% ethanol. Set up video equipment to the side such that the whole box is in the viewing field. Keep the set up and surroundings the same each day to avoid introducing novelty.
3. Remove one weanling from the cage and place in a clean holding cup. Record weight.
4. Begin video recording by filming the test identification card, with mouse identification number, age and date of testing. Transfer mouse from holding cup to the center square. Time for three minutes, counting the number of lines traversed by both front paws of the mouse during the test.
5. Return mouse to a clean cage and end video recording.
6. Clean the testing apparatus with 70% ethanol.
7. Repeat until all litter is tested, then return all pups to the home cage.
8. Clean all testing equipment with 70% ethanol.
9. Using the videos, quantitate the number of rearing events by tallying after visual observation, where a mouse stands with both front paws clear of support, and grooming events, where both front paws are engaged in cleaning.

3. Wire Mesh Grip Strength Test
Note: The grip strength test is conducted on alternate days between P22 and P26, to assess neuromuscular strength.
1. Transport mice to testing area and allow to rest in home cage for 30 min before testing.
2. Prepare apparatus by cleaning a Plexiglass box and mesh grid with 70% ethanol. Place bubble wrap in the bottom of the box and cover with paper.
3. Separate mice into groups of three, placing in individual holding cups.
4. Place first mouse onto the center of the wire mesh and slowly invert 10-20 cm above the soft surface in the bottom of the Plexiglass box. Measure the latency to fall using a stopwatch. Terminate testing after 60 sec have elapsed if the mouse does not fall.
5. Return mouse to holding cup, wipe mesh with 70% ethanol and replace paper over the bubble wrap. Conduct the test on the remaining two mice in the group before returning to the first. Repeat until each mouse has been tested a total of three times.
6. Return the group to a clean cage and continue with remaining groups. If there are fewer than three mice in any group, ensure that a 5 min inter-trial recovery interval is allowed.
7. Return all mice to the home cage, dispose of paper and clean testing equipment with 70% ethanol.

2. Examination of Retinal Structure

1. Anaesthetize animals at P30-35 by intraperitoneal injection of ketamine (100 mg/kg) and xylazine (10 mg/kg). Assess depth of anesthesia by pinching the footpad and proceed only in the absence of a response, in line with IACUC guidelines. Perfuse with 4% PFA/PBS[48].
2. To remove the eyes, clean the skin at the incision site with 70% ethanol, before cutting through the skin at the base of the skull. Peel back the skin to expose the skull and clean with 70% ethanol. Using clean instruments, carefully cut through the skull to reach the eye sockets and expose the eyes. Sever the optic nerve, gently remove the eye from the socket and rinse in PBS.
3. Fix eyes in 4% PFA/PBS for 10 min at room temperature.
4. Place eyes in a small petri dish containing PBS. Make a small incision in the center of the cornea using stitch removal scissors. Remove the cornea by cutting the edge between the cornea and sclera. Use forceps to remove the iris. Finally, peel off the RPE layers, leaving the retina intact and the lens in place.
Note: The 4% PFA/PBS fixation will cause RPE detachment allowing for the RPE to be easily peeled from the outside of the retina.
5. Re-fix in 4% PFA/30% sucrose/PBS for 15 min at room temperature before returning the eye to a petri dish containing PBS. Pull out the lens using forceps, bringing the vitreous body along with it.
6. Cryoprotect in 30% sucrose overnight at 4 °C.
7. Coat eyes in Optimum Cutting Temperature compound (OCT) and transfer to an embedding mold containing fresh OCT. Orient the eye such that the sagittal plane is parallel with the cutting face, using as few movements as possible and avoiding the introduction of air bubbles. Flash freeze by immersing the mold in a dry ice/ethanol bath. Store blocks at -80 °C.
8. Using a cryostat, cut 20 µm sagittal sections and collect on precleaned slides.
9. Stain sections with hematoxylin and eosin according to standard protocols[49]. Image using a light microscope equipped for bright field microscopy.

3. Histochemical Staining

1. Sample Preparation
1. Euthanize animals at P30-35 using isoflurane overdose (30% in propylene glycol) via open drop inhalation. Assess euthanasia by the cessation of breathing, heartbeat and lack of response to pinching the footpad. Confirm death by cervical dislocation and organ removal, in line with IACUC guidelines.
2. To remove the brain, clean the skin at the incision site with 70% ethanol, before cutting through the skin at the base of the skull. Peel back the skin to expose the skull and clean with 70% ethanol. Using clean instruments, carefully cut through the skull and remove to expose the brain. Remove the membranes, and gently remove the brain from the skull cavity. Rinse in PBS.

3. Coat the brain in OCT and transfer to an embedding mold containing fresh OCT. Orient the brain such that the sagittal plane is parallel with the cutting face, using as few movements as possible and avoiding the introduction of air bubbles. Flash freeze by immersing the mold in a dry ice/ethanol bath and store at -80 °C.
4. Using a cryostat, cut 10 µm sagittal sections and collect on precleaned slides.

2. NADH Diaphorase Staining
   1. Prepare 0.05 M Tris buffer, pH 7.6 by dissolving 5.72 g Tris-HCl and 1.66 g Tris base in 1L-deionized water. Store at 4 °C for up to six weeks.
   2. Prepare NADH solution (2.25 mM NADH in 0.05 M Tris buffer). Aliquot and store at -20 °C.
   3. Prepare NBT solution (2.5 mM Nitro-Blue Tetrazolium in 0.05 M Tris buffer). Store at 4 °C for up to six weeks in a glass bottle.
   4. Combine equal volumes of NADH solution and NBT solution to make staining solution and add 1 ml to each slide. Incubate at 37 °C in a humidified chamber for 30 min.
   5. Aspirate staining solution and wash three times with dH_2O.
   6. Wash three times each in ascending and descending concentrations of acetone/dH_20 (30%, 60%, 90%, 60%, 30%) for 2 min at room temperature.
   7. Rinse three times in dH_2O and mount sections with aqueous medium. Image using a light microscope equipped for bright field microscopy. Blue staining corresponds to enzymatic activity.

3. Succinate Dehydrogenase Histochemical Staining
   1. Prepare 0.2 M sodium monobasic phosphate/dH_2O and 0.2 M sodium dibasic phosphate/dH_2O.
   2. Make 0.2 M phosphate buffer, pH 7.6 by combining 3 parts monobasic phosphate with 20 parts sodium dibasic phosphate.
   3. Prepare staining solution (0.1 M sodium succinate, 1.25 M NBT in 0.2 M phosphate buffer) and add 1 ml to each slide. Incubate at 37 °C in a humidified chamber for 60 min.
   4. Aspirate staining solution and wash three times in dH_2O.
   5. Wash three times each in ascending and descending concentrations of acetone/dH_2O (30%, 60%, 90%, 60%, 30%) for 2 min at room temperature.
   6. Rinse three times in dH_2O and mount sections with aqueous medium. Image using a light microscope equipped for bright field microscopy. Blue staining corresponds to enzymatic activity.

Representative Results

This section describes examples of the results obtainable using these methods. In the hind-limb test, the number of pull attempts made and the latency to fall are summed over two consecutive tests for each day. This test can be used to compare genetically different groups to distinguish mice with reduced neuromuscular strength. *HtrA2*^{tm1jhoh} (HTRA2 KO) mice in **Figure 1A**-**B** demonstrate no change in the number of pulls and latency to fall from P4-6 followed by a reduction in neuromuscular strength at P7-10, as compared to littermates (HTRA2 WT). The expected increase in strength with age is also observable in the wild-type animals. For the weanling observation test, total activity can be evaluated by summing all events (lines traversed, rearing and grooming events), averaged across the three consecutive days of testing. Alternatively, each specific type of event can be individually analyzed. Here representative results are presented, demonstrating reduced activity of HTRA2 KO mice compared to WT littermates. These data demonstrate that total activity can be quantitatively measured and compared across groups (**Figure 1C**). It is also possible to quantify differences in grip strength by calculating a daily average from the three repeats performed on each testing day. When HTRA2 KO mice are compared to littermate controls, reductions in strength manifest in a shorter latency to fall (**Figure 1D**).

H&E staining of the retina generates images in which retinal structure can be examined and compared (**Figure 2**). The layers of cell types that compose the retina are clearly delineated allowing comparison between genetic groups. Here, *HtrA2*^{tm1jhoh};*HtrA3*^{tm1jhoh} mice show no changes in retinal structure, compared to *HtrA2*^{WT};*HtrA3*^{tm1jhoh} mice at P35. Finally, histochemical staining for electron transport chain complex activity can be used to identify changes in respiratory enzyme functions, with increases in staining intensity reflecting increase enzyme activity, such as the reduction observed in the cerebellum and striatum of *HtrA2*$^{flox/flox}$;Tg(Nes-cre)1Kln/J (NesKO) brain when compared to WT littermates (**Figure 3**).

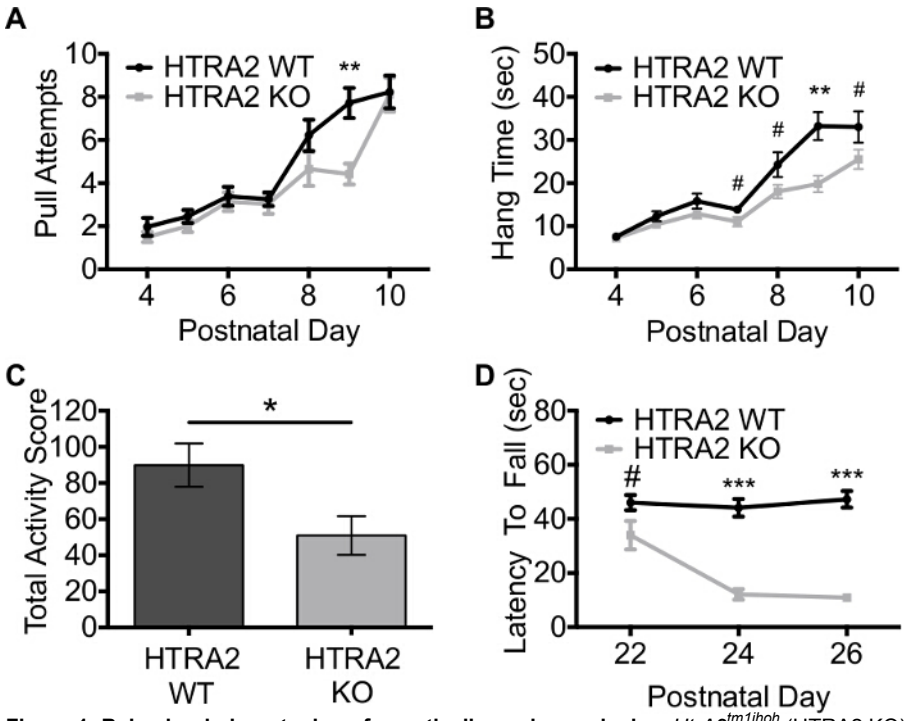

Figure 1: Behavioral phenotyping of genetically engineered mice. *HtrA2*^{tm1jhoh} (HTRA2 KO) mice were subjected to the described behavioral testing and compared to wildtype (HTRA2 WT) littermate controls. (**A**-**B**) The hind limb suspension test was performed on WT and KO neonates from P4-P10 and demonstrates a reduction in neuromuscular strength in KO animals (WT: n = 28, KO: n = 19). (**A**) KO pups initially make a similar number of pull attempts as WT siblings, but show a decrease in attempts made at later time points. (**B**) KO neonates' latency to fall is also initially normal but decreases from P7 onwards. (**C**) The weanling observation total activity score was reduced in KO animals compared to WT littermates, consistent with reduced activity of these mice (WT: n = 19, KO: n = 12). (**D**) KO animals also had a reduced latency to fall during the mesh inversion test, demonstrating reduced grip strength of HTRA2 KO mice (WT: n = 17, KO: n = 9). Data represents Mean ± SEM (# 0.1 <p <0.05, *p <0.05, **p <0.001, ***p <0.001 by independent t-tests). This figure has been modified from Patterson *et al.*[34] Please click here to view a larger version of this figure.

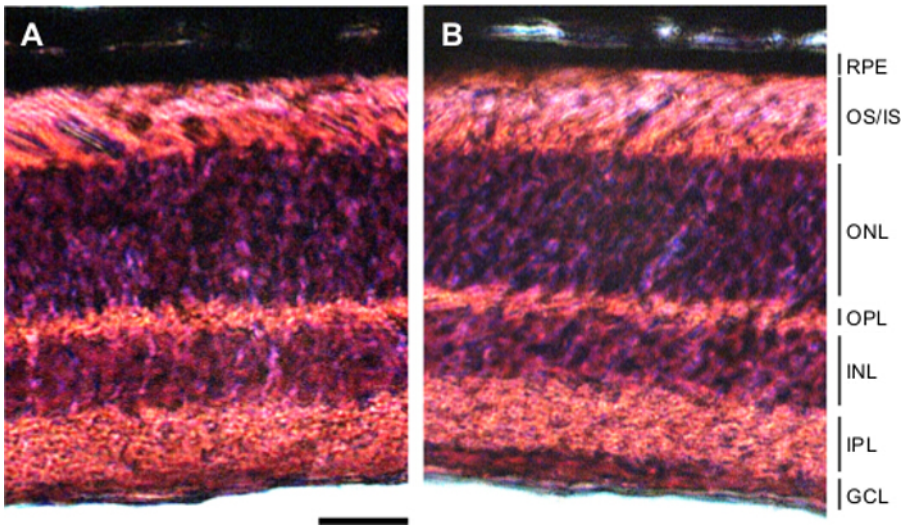

Figure 2: H&E staining of retina. Staining retinal sections with hematoxylin and eosin allows examination of structure, delineating the retinal layers. Here sections from P35 *HtrA2*^{WT};*HtrA3*^{tm1jhoh} (**A**) and *HtrA2*^{tm1jhoh};*HtrA3*^{tm1jhoh} (**B**) display normal retinal structure. RPE: retinal pigment epithelium, OS: outer segments, IS:inner segments, ONL: outer nuclear layer, OPL: outer plexiform layer, INL: inner nuclear layer, IPL: inner plexiform layer, GCL; ganglion cell layer. Scale bar = 1 mm. Please click here to view a larger version of this figure.

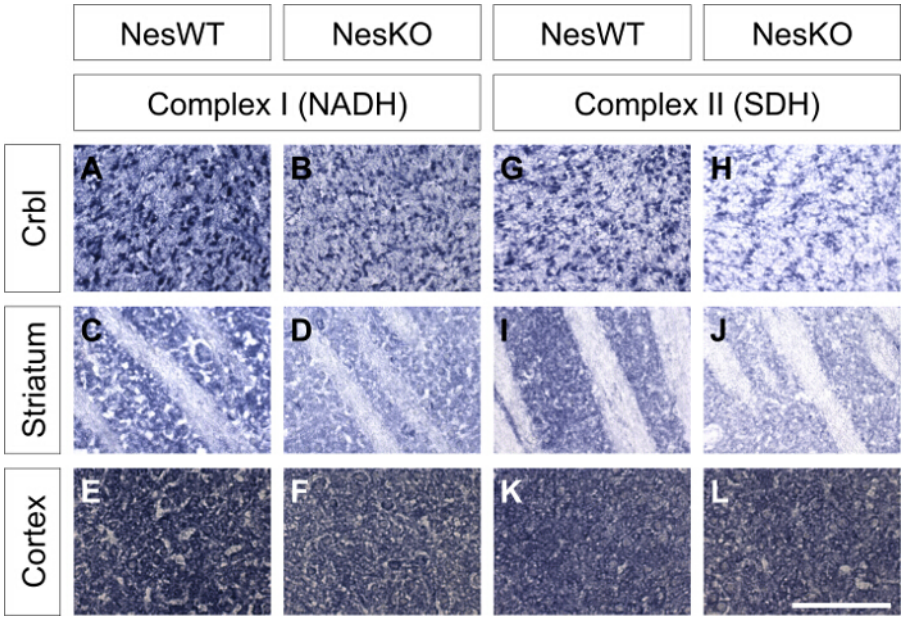

Figure 3: Respiratory complex activity. Histochemical staining for NADH diaphorase (complex I) and succinate dehydrogenase (complex II) activity was performed on transverse brain sections of P25 *HtrA2*$^{flox/flox}$;Tg(Nes-cre)1Kln/J (NesKO) and *HtrA2*$^{+/flox}$;Tg(Nes-cre)1Kln/J (NesWT) littermates. NADH diaphorase enzyme activity is decreased in cerebellum (Crbl, **B**) and striatum (**D**) of NesKO brain compared to NesWT controls (**A**, **C**), but not in cerebral cortex (**E**-**F**). SDH activity is similarly reduced in cerebellum and striatum of NesKO mice (**H**, **J**) compared to NesWT controls (**G**, **I**) but there is no change in cerebral cortex (**K**-**L**). Scale bar = 200 µm. This figure has been modified from Patterson *et al.*[34] Please click here to view a larger version of this figure.

Discussion

Robust treatments are needed to limit the impact of debilitating conditions related to human aging, but they remain elusive for many conditions. To identify potential therapeutic targets and develop strategies for intervention, the causes and pathology of diseases associated with aging must first be understood. Not all genetically modified mice immediately present with clear phenotypes that are related to the disease of interest, even if those genes have previously been linked to the condition in human studies. Therefore more systematic investigations are required and genetically modified mice should be subjected to appropriate experiments to identify phenotypes that may be related to the associated diseases in humans.

Myriad behavioral tests exist to assay neurological function in mice[50,51]. The behavioral tests outlined herein are suited to the hypothesized phenotypes based on human findings and the actual phenotypes observed in mice. In addition, these tests are simple to perform in laboratories with little or even no experience in conducting behavioral experiments. There is no requirement for sophisticated equipment but the results are meaningful and informative when properly collected, making them useful as a first step in examining the phenotype of genetically modified mice that are expected to have neuromuscular defects. The resultant data can then be used to direct the focus of further testing, potentially with more sophisticated testing apparatus.

Similarly, many techniques exist for assessing respiratory function in tissues[52]. Measuring the rate of ATP synthesis, oxygen consumption or changes in mitochondrial membrane potential are important readouts of mitochondrial function but they can be complicated and time consuming to perform, requiring specific reagents and equipment[52-55]. In addition, they are often limited to the level of the mitochondrion or cell, relying on cultured cells, lysates or isolated mitochondria. Histochemical staining is a useful first step in identifying mitochondrial dysfunction without a large investment of time or resources. Moreover, the ability to stain tissue sections lends itself to quickly identifying regional differences that might not be as apparent with other techniques, for example the area-specific loss of enzymatic staining observed in HtrA2-deficient brain. While the technique is limited in its ability to measure fold changes in respiratory capacity, it maps out defined brain regions that can then be pursued using more complex methods.

While the techniques presented within this phenotyping schedule are simple to conduct, performing certain steps properly is critical to the success of the experiments. For the behavioral phenotyping, great care must be taken to ensure tests are performed at the same time and in the same location each day to limit variation introduced by the novelty of location or by the difference in the circadian rhythm. The equipment should be organized in the same way each day for similar reasons. The room organization is especially critical for the activity test, where small changes in novelty can greatly influence the activity of the mouse. When measuring grip strength, investigators should ascertain that mice have a proper hold of the mesh before inversion. Similarly, care must be taken to properly suspend the pup before releasing in the hind limb test or the test results will be skewed towards a shorter latency to fall.

For tissue phenotyping, obtaining good sections is vital. Informative staining of the retina depends upon effective fixation before dissection or artifacts will arise during sectioning and dissection and distort the morphology. Histochemical staining requires brains to be frozen quickly after dissection to preserve enzyme function, but the incubation time is similarly critical; small fluctuations in temperature or in the length of time can cause differences in the staining intensity. Where possible, samples should be processed at the same time to allow comparison between groups.

Here a testing regimen used to study genetically modified mice expected to display subtle phenotypes associated with age-related diseases, namely AMD and PD, is described. This phenotyping schedule can be used to identify deficits in neuromuscular strength and activity, as well as identify structural and functional defects within the tissues of interest. This schedule provides a systematic analysis of early phenotypes in young, genetically altered mice. In the future, this method can be applied to any genetically modified mice expected to present with an AMD or PD related phenotype, as well as those of unknown etiology that appear overtly normal. The simplicity of the tests allows testing without significant investment but can be used to inform further studies. By combining behavioral testing with cellular phenotyping, it is possible to limit the number of mice used and directly compare animal performance with the physiological condition. This phenotyping schedule provides an initial analysis that can be used to direct the focus of subsequent studies.

Disclosures

The authors have no competing interests to disclose.

Acknowledgements

Funding for this research came from Rosebay Medical Foundation and a Yale Medical School Dean's Research Fund (JH). We thank Dr. Claire Koenig for help with behavioral experiments. Genetically engineered mouse lines were generated at Ozgene (Perth, Australia).

References

1. Klein, R. J. *et al.* Complement factor H polymorphism in age-related macular degeneration. *Science* **308**, 385-389 (2005).
2. Zareparsi, S. *et al.* Strong association of the Y402H variant in complement factor H at 1q32 with susceptibility to age-related macular degeneration. *Am J Hum Genet* **77**, 149-153 (2005).
3. Yang, Z. *et al.* A variant of the HTRA1 gene increases susceptibility to age-related macular degeneration. *Science* **314**, 992-993 (2006).
4. Dewan, A. *et al.* HTRA1 promoter polymorphism in wet age-related macular degeneration. *Science* **314**, 989-992 (2006).
5. Francis, P. J., Zhang, H., Dewan, A., Hoh, J., & Klein, M. L. Joint effects of polymorphisms in the HTRA1, LOC387715/ARMS2, and CFH genes on AMD in a Caucasian population. *Mol Vis.* **14**, 1395-1400 (2008).
6. Cameron, D. J. *et al.* HTRA1 variant confers similar risks to geographic atrophy and neovascular age-related macular degeneration. *Cell Cycle* **6**, 1122-1125 (2007).
7. Herbert, A. P. *et al.* Structure shows that a glycosaminoglycan and protein recognition site in factor H is perturbed by age-related macular degeneration-linked single nucleotide polymorphism. *J Biol Chem* **282**, 18960-18968 (2007).
8. Ding, J. D. *et al.* Expression of human complement factor h prevents age-related macular degeneration-like retina damage and kidney abnormalities in aged cfh knockout mice. *Am J Pathol* **185**, 29-42 (2015).
9. Nakayama, M. *et al.* Overexpression of HtrA1 and exposure to mainstream cigarette smoke leads to choroidal neovascularization and subretinal deposits in aged mice. *Invest Ophthalmol Vis Sci* **55**, 6514-6523 (2014).
10. Liu, J., & Hoh, J. Postnatal overexpression of the human ARMS2 gene does not induce abnormalities in retina and choroid in transgenic mouse models. *Invest Ophthalmol Vis Sci.* **56**, 1387-1388 (2015).
11. Kanda, A. *et al.* A variant of mitochondrial protein LOC387715/ARMS2, not HTRA1, is strongly associated with age-related macular degeneration. *Proc Natl Acad Sci U S A* **104**, 16227-16232 (2007).
12. Zumbrunn, J., & Trueb, B. Primary structure of a putative serine protease specific for IGF-binding proteins. *FEBS Lett.* **398**, 187-192 (1996).
13. Clausen, T., Southan, C., & Ehrmann, M. The HtrA family of proteases: implications for protein composition and cell fate. *Mol Cell.* **10**, 443-455 (2002).
14. Nie, G. Y., Hampton, A., Li, Y., Findlay, J. K., & Salamonsen, L. A. Identification and cloning of two isoforms of human high-temperature requirement factor A3 (HtrA3), characterization of its genomic structure and comparison of its tissue distribution with HtrA1 and HtrA2. *Biochem J.* **371**, 39-48 (2003).
15. Runyon, S. T. *et al.* Structural and functional analysis of the PDZ domains of human HtrA1 and HtrA3. *Protein Sci.* **16**, 2454-2471 (2007).
16. Glaza, P. *et al.* Structural and Functional Analysis of Human HtrA3 Protease and Its Subdomains. *PLoS One.* **10**, e0131142 (2015).
17. Dolmans, D. E., Fukumura, D., & Jain, R. K. Photodynamic therapy for cancer. *Nat Rev Cancer.* **3**, 380-387 (2003).
18. Grau, S. *et al.* Implications of the serine protease HtrA1 in amyloid precursor protein processing. *Proc Natl Acad Sci U S A.* **102**, 6021-6026 (2005).
19. Lecha, M., Puy, H., & Deybach, J. C. Erythropoietic protoporphyria. *Orphanet J Rare Dis.* **4**, 19 (2009).
20. Ethirajan, M., Chen, Y., Joshi, P., & Pandey, R. K. The role of porphyrin chemistry in tumor imaging and photodynamic therapy. *Chem Soc Rev.* **40**, 340-362 (2011).
21. Li, W. *et al.* Structural insights into the pro-apoptotic function of mitochondrial serine protease HtrA2/Omi. *Nat Struct Biol* **9**, 436-441 (2002).
22. Jo, H., Patterson, V., Stoessel, S., Kuan, C. Y., & Hoh, J. Protoporphyrins enhance oligomerization and enzymatic activity of HtrA1 serine protease. *PLoS One.* **9**, e115362 (2014).
23. Bogaerts, V. *et al.* Genetic variability in the mitochondrial serine protease HTRA2 contributes to risk for Parkinson disease. *Hum Mutat* **29**, 832-840 (2008).
24. Baldi, A. *et al.* The HtrA1 serine protease is down-regulated during human melanoma progression and represses growth of metastatic melanoma cells. *Oncogene* **21**, 6684-6688 (2002).
25. Oka, C. *et al.* HtrA1 serine protease inhibits signaling mediated by Tgfbeta family proteins. *Development* **131**, 1041-1053 (2004).
26. Chien, J. *et al.* A candidate tumor suppressor HtrA1 is downregulated in ovarian cancer. *Oncogene* **23**, 1636-1644 (2004).
27. Grau, S. *et al.* The role of human HtrA1 in arthritic disease. *J Biol Chem* **281**, 6124-6129 (2006).
28. Chien, J. *et al.* Serine protease HtrA1 modulates chemotherapy-induced cytotoxicity. *J Clin Invest* **116**, 1994-2004 (2006).
29. Chien, J., Campioni, M., Shridhar, V., & Baldi, A. HtrA serine proteases as potential therapeutic targets in cancer. *Curr Cancer Drug Targets.* **9**, 451-468 (2009).
30. Hara, K. *et al.* Association of HTRA1 mutations and familial ischemic cerebral small-vessel disease. *N Engl J Med* **360**, 1729-1739 (2009).

31. Jones, A. *et al.* Increased expression of multifunctional serine protease, HTRA1, in retinal pigment epithelium induces polypoidal choroidal vasculopathy in mice. *Proc Natl Acad Sci U S A* **108**, 14578-14583 (2011).
32. Vierkotten, S., Muether, P. S., & Fauser, S. Overexpression of HTRA1 leads to ultrastructural changes in the elastic layer of Bruch's membrane via cleavage of extracellular matrix components. *PLoS One.* **6**, e22959 (2011).
33. Strauss, K. M. *et al.* Loss of function mutations in the gene encoding Omi/HtrA2 in Parkinson's disease. *Hum Mol Genet* **14**, 2099-2111 (2005).
34. Patterson, V. L. *et al.* Neural-specific deletion of Htra2 causes cerebellar neurodegeneration and defective processing of mitochondrial OPA1. *PLoS One* **9**, e115789 (2014).
35. Jones, J. M. *et al.* Loss of Omi mitochondrial protease activity causes the neuromuscular disorder of mnd2 mutant mice. *Nature* **425**, 721-727 (2003).
36. Martins, L. M. *et al.* Neuroprotective role of the Reaper-related serine protease HtrA2/Omi revealed by targeted deletion in mice. *Mol Cell Biol* **24**, 9848-9862 (2004).
37. Kang, S. *et al.* Loss of HtrA2/Omi activity in non-neuronal tissues of adult mice causes premature aging. *Cell Death Differ* **20**, 259-269 (2013).
38. Dynon, K. *et al.* HtrA3 as an early marker for preeclampsia: specific monoclonal antibodies and sensitive high-throughput assays for serum screening. *PLoS One* **7**, e45956 (2012).
39. Singh, H. *et al.* HtrA3 Is Downregulated in Cancer Cell Lines and Significantly Reduced in Primary Serous and Granulosa Cell Ovarian Tumors. *J Cancer* **4**, 152-164 (2013).
40. Inagaki, A. *et al.* Upregulation of HtrA4 in the placentas of patients with severe pre-eclampsia. *Placenta* **33**, 919-926 (2012).
41. Liu, J., Li, Y. and Hoh, J. Generation and characterization of mice with a conditional null allele of the HtrA4 gene. *Mol Med Rep.* (2015).
42. Bowden, M. A., Di Nezza-Cossens, L. A., Jobling, T., Salamonsen, L. A., & Nie, G. Serine proteases HTRA1 and HTRA3 are down-regulated with increasing grades of human endometrial cancer. *Gynecol Oncol.* **103**, 253-260 (2006).
43. Chen, Y. Y. *et al.* Functional antagonism between high temperature requirement protein A (HtrA) family members regulates trophoblast invasion. *J Biol Chem* **289**, 22958-22968 (2014).
44. Fritsche, L. G. *et al.* Age-related macular degeneration is associated with an unstable ARMS2 (LOC387715) mRNA. *Nat Genet* **40**, 892-896 (2008).
45. Beleford, D., Rattan, R., Chien, J., & Shridhar, V. High temperature requirement A3 (HtrA3) promotes etoposide- and cisplatin-induced cytotoxicity in lung cancer cell lines. *J Biol Chem.* **285**, 12011-12027 (2010).
46. Hegde, R. *et al.* Identification of Omi/HtrA2 as a mitochondrial apoptotic serine protease that disrupts inhibitor of apoptosis protein-caspase interaction. *J Biol Chem* **277**, 432-438 (2002).
47. Martins, L. M. *et al.* The serine protease Omi/HtrA2 regulates apoptosis by binding XIAP through a reaper-like motif. *J Biol Chem* **277**, 439-444 (2002).
48. Gage, G. J., Kipke, D. R., & Shain, W. Whole animal perfusion fixation for rodents. *J Vis Exp.* (2012).
49. Fischer, A. H., Jacobson, K. A., Rose, J., & Zeller, R. Hematoxylin and eosin staining of tissue and cell sections. *CSH Protoc.* **2008**, pdb prot4986 (2008).
50. Wahlsten, D. A developmental time scale for postnatal changes in brain and behavior of B6D2F2 mice. *Brain Res.* **72**, 251-264 (1974).
51. El-Khodor, B. F. *et al.* Identification of a battery of tests for drug candidate evaluation in the SMNDelta7 neonate model of spinal muscular atrophy. *Exp Neurol* **212**, 29-43 (2008).
52. Brand, M. D., & Nicholls, D. G. Assessing mitochondrial dysfunction in cells. *Biochem J.* **435**, 297-312 (2011).
53. Chance, B., Williams, G. R., Holmes, W. F., & Higgins, J. Respiratory enzymes in oxidative phosphorylation. V. A mechanism for oxidative phosphorylation. *J Biol Chem.* **217**, 439-451 (1955).
54. Kamo, N., Muratsugu, M., Hongoh, R., & Kobatake, Y. Membrane potential of mitochondria measured with an electrode sensitive to tetraphenyl phosphonium and relationship between proton electrochemical potential and phosphorylation potential in steady state. *J Membr Biol.* **49**, 105-121 (1979).
55. Brown, G. C., & Brand, M. D. Proton/electron stoichiometry of mitochondrial complex I estimated from the equilibrium thermodynamic force ratio. *Biochem J.* **252**, 473-479 (1988).

